general, however, the agreement between the present data and major features of the Lomer model is quite satisfying.

V. CONCLUSIONS

High-frequency magnetoacoustic data have been obtained for very pure tungsten. From the observed oscillatory behavior, the extremal dimensions of the Fermi surface have been obtained. The resulting shape of the Fermi surface is in qualitative agreement with the theoretical model of Lomer. Estimates of the extremal areas along certain symmetry directions are in reasonable accord with those found from high-field de Haas-van Alphen data.

ACKNOWLEDGMENTS

Thanks are due to H. Sell of the Westinghouse Lamp Division, Bloomfield, New Jersey for providing the high-purity samples of tungsten used in this work. The author would like to express his appreciation to R. Farich for his great care in grinding and polishing the acoustic specimens.

PHYSICAL REVIEW VOLUME 133, NUMBER 4A 17 FEBRUARY 1964

Spin Temperature in Nuclear Double Resonance*

FRED M. LURIE† AND CHARLES P. SLICHTER
Department of Physics, University of Illinois, Urbana, Illinois
(Received 7 October 1963)

A magnetic double resonance technique is described which allows the strong resonance of one nuclear species to be used to detect the much weaker resonance of a second species. Based on the proposal of Hartmann and Hahn, the new technique is experimentally simpler, and involves no critical adjustments of experimental parameters. It involves the method of adiabatic demagnetization in the rotating reference frame. The theoretical interpretation is an adaptation of Redfield's thermodynamic approach, performed in a specially chosen reference system. The technique and theory are verified quantitatively in lithium metal using the strong resonance of the 92.6% abundant Li^7 at 15 Mc/sec to detect the much weaker resonance of the 7.4% abundant Li^6 at 5.679 Mc/sec.

I. INTRODUCTION

SEVERAL years ago, Hartmann and Hahn[1] made a brilliant suggestion for a new type of double resonance which promised to provide greatly increased sensitivity in the detection of otherwise weak resonances. The technique enables one to use the strong resonance of one spin system to detect the weak resonance of a second one. If two nuclear species of spin I and S and gyromagnetic ratios γ_I and γ_S were simultaneously present, acted on by rotating fields $(H_1)_I$ and $(H_1)_S$ tuned to the respective resonances, Hartmann and Hahn's double resonance occurred when

$$\gamma_I(H_1)_I=\gamma_S(H_1)_S. \quad (1)$$

They showed that when this condition was satisfied, the two spin systems were strongly coupled even though the precession frequencies in the static field H_0 were at widely different frequencies. The coupling occurs via the dipolar interaction between the I and S spins. Crudely speaking, we may say the precession of the S spins about their H_1 causes the component of the dipolar field along the direction of the static field H_0 to oscillate at an angular frequency $\gamma_S(H_1)_S$. When the Hahn condition is satisfied, the frequency of alternation is just such as to induce transitions of the I spins relative to their rotating field $(H_1)_I$. Hahn showed that fairly rapid phase changes of the alternating field $(H_1)_S$ would, through this coupling, produce a saturation of the I spins. In this way, even though the S resonance might be hard to observe directly, it could be seen indirectly by its effect on the I spins. Exactly how the method works has been explained in full detail by Hartmann and Hahn.[2] However, the analysis is necessarily rather formidable and cannot, in fact, be carried through completely since an inherent feature of their theory is a calculation of a cross-relaxation time between the two species. In their paper, they also describe the exact sequence of pulses necessary to bring about the double resonance, and they demonstrate the effect.

In our paper, we describe a modification of Hartmann and Hahn's experiment.[3] Our modifications bring about important simplifications in the experimental technique

* This research supported in part by a grant from the U. S. Atomic Energy Commission.
† Present address: the Department of Physics, University of Pennsylvania, Philadelphia, Pennsylvania. This paper is based on the Ph.D. thesis presented by Dr. Lurie at the University of Illinois.
[1] S. R. Hartmann and E. L. Hahn, Bull. Am. Phys. Soc. **5**, 498 (1960).
[2] S. R. Hartmann and E. L. Hahn, Phys. Rev. **128**, 2042 (1962).
[3] F. M. Lurie and C. P. Slichter, Phys. Rev. Letters **10**, 403 (1963).

and make the theoretical analysis not only simpler but, in fact, capable of exact solution.

As will become apparent, the two different techniques have simple analogies in thermodynamics. Consider two bodies connected by a rod to provide thermal contact. One body, of small heat capacity, represents the low abundance S spins, the other of large heat capacity, represents the I spins. Hartmann and Hahn's experiments are analogous to heating the large object by holding the small one at constant elevated temperature. The rate of heating depends on the thermal conductivity of the rod, and the heat capacity of the large object (the I-spin system), but is independent of the heat capacity of the small object (the S-spin system) since we never let its temperature change. A theoretical prediction of the rate of heating of the large object would require knowledge of its heat capacity and of the thermal conductivity of the rod. In resonance language, that means we must calculate a cross-relaxation time. This cannot be done exactly.

Our experiment is analogous to breaking the thermal contact between the rod and the small object, heating the small object to a known temperature, disconnecting the heater, and reconnecting the rod. After a sufficiently long time, the entire system of large object, small object, and rod, come to a common temperature. Since the S system has a relatively small heat capacity, the final temperature is not much different from the initial temperature of the large object. However, we can repeat the cycle. In fact, if we do the thermal mixing N times, the heating of the I system is as great as it would be for a single mixing with an S system whose heat capacity is N times larger than it actually is. Since N may be made very large, a significant effect can be achieved even when the S spins have a very small relative heat capacity.

Calculation of the temperature rise requires knowledge only of the heat capacities of the parts. It is not even necessary for the heat capacity of the rod to be small since we can easily include its effect. Calculation of the heat capacities of the spin systems is simple and can be done exactly. We therefore have a simple, exact theory to compare with experiment.

As we shall see (and as Hahn and Hartmann's analysis shows), the effective thermal conductivity of the rod depends on the size of the two rotating fields. The Hahn condition provides the fastest mixing or largest thermal conductivity. The heat capacity of the two systems is determined in large measure by the strength of the H_1's. We can therefore vary the heat capacities experimentally although we must remember that when the H_1 ratio does not satisfy the Hahn condition, it may take a longer time for a uniform temperature to be reached. The dipolar coupling between the two different species provides the thermal contact or "rod." As we have remarked, we can easily calculate its heat capacity. Likewise, there is a contribution to the heat capacity from the dipolar coupling of the I spins among themselves and the S spins among themselves. All these effects can be rigorously and simply included. In the process, we shall demonstrate that it is not necessary for the H_1's to be large compared to the local fields and we even demonstrate the coupling in cases where $(H_1)_I$ has been turned to zero.

It will come as no surprise to the reader that the analysis we have just given is based on Redfield's[4] concept of a spin temperature in the rotating reference frame. In our experiments, the concept is applied to two rotating frames simultaneously. Although such a procedure may sound formidable, the formal mathematics is quite simple.

Our experiments were performed on lithium metal. The I system was the 92.6% abundant isotope Li^7 whose strong resonance we observed directly. The S spins were the 7.4% abundant isotope Li^6. Since both resonances have been thoroughly studied in metallic lithium by Holcomb and Norberg,[5] we learn nothing new about either the nuclei or the metal. However, such a well-understood system is ideal for a test of the double resonance theory. We performed some measurements at liquid nitrogen temperature, but the bulk of the data was obtained at 1.5°K where the long nuclear relaxation times (30 sec for Li^7 and longer for Li^6) make it simple to obtain isolation from the influence of the lattice for the duration of the experiment. A magnetic field of 9062 G was used for all experiments.

The basic experiments on which this work is based are those in which Redfield discovered the need for the concept of spin temperature in the rotating reference frame. Shortly thereafter, Bloembergen and Sorokin[6] performed double resonance experiments, demonstrating what they called the transverse Overhauser effect in which the resonance of one nuclear species polarized the nuclei of a second species. They also showed how the spin-lattice relaxation of one species affected the transverse relaxation time T_2 of a second species. Goldman and Landesman[7] demonstrated spin mixing between two species under the influence of an alternating field when one species had a large quadrupole splitting. Hahn[1] proposed his double resonance technique, which he and Hartmann[8] have subsequently verified in detail. Further single resonance experiments by Goldburg,[9] Slichter and Holton,[10] and more recently Hartmann and Anderson; Holcomb, Pedersen, and Sliker; and Solomon and Ezratty[11] have studied further

[4] A. G. Redfield, Phys. Rev. **98**, 1787 (1955).
[5] D. F. Holcomb and R. E. Norberg, Phys. Rev. **98**, 1074 (1955).
[6] N. Bloembergen and P. Sorokin, Phys. Rev. **110**, 865 (1958).
[7] M. Goldman and M. Landesman, Compt. Rend. **252**, 263 (1961).
[8] S. R. Hartmann and E. L. Hahn, Phys. Rev. **128**, 2042 (1962).
[9] Walter I. Goldburg, Phys. Rev. **122**, 831 (1961); also **128**, 1554 (1962).
[10] C. P. Slichter and W. C. Holton, Phys. Rev. **122**, 1701 (1961).
[11] A. G. Anderson and S. R. Hartmann, Phys. Rev. **128**, 2023 (1962); I. Solomon and J. Ezratty, *ibid.* **127**, 78 (1962); D. F. Holcomb, B. Pedersen, and T. Sliker, *ibid.* **123**, 1951 (1961).

aspects of the spin temperature concept. Redfield and Provotorov[12] have made further theoretical studies.

Recently, Redfield[13] has successfully applied the Hahn double resonance method to study quadrupole splittings, using a field cycling technique. It was interest in Redfield's experiments that stimulated us to undertake the work described in this paper.

In Sec. II, we outline our basic experimental procedure. In Sec. III, we develop the theoretical analysis. We give the details of the apparatus in Sec. IV, and the experimental results in Sec. V. We present an approximate calculation of the cross-relaxation time in the Appendix.

II. EXPERIMENTAL PROCEDURE

The theoretical analysis of our experiment is simplest if we have before us an outline of the various steps in the experiment. In this section, we give such an outline.

We start with the static field H_0 at a value H_{00}. The two rotating fields, when turned on, are adjusted to rotate at frequencies ω_I and ω_S given, respectively, by

$$\begin{aligned}\gamma_1 H_{00}&=\omega_I,\\ \gamma_S H_{00}&=\omega_S,\end{aligned} \tag{2}$$

that is, the two nuclear species are simultaneously at resonance when $H_0=H_{00}$.

We start at $t=0$, with the two nuclear spin systems magnetized to thermal equilibrium at the lattice temperature, their magnetization vectors pointing along H_0 and with the two H_1's zero. Our first step involves turning on $(H_1)_I$ in such a manner that $\mathbf{M}_I$ is brought to point along $(H_1)_I$ in the I system rotating reference frame. This frame, of course, is the one which, relative to the laboratory, rotates about the H_0 axis at frequency ω_I in the same sense as the nuclear precession of the I spins. If we simply turned on $(H_1)_I$, we would fail in our objective since, as shown in Ref. 10, $\mathbf{M}_I$ would precess around it in the rotating frame, always remaining perpendicular and decaying in amplitude in a few hundred microseconds [$(T_2)_I$, the T_2 of the I spins]. In order to get $\mathbf{M}_I$ parallel to $(H_1)_I$, we therefore first displace H_0 from H_{00} by an amount $h_0 \gg (H_1)_I$. Then $(H_1)_I$ is turned on. The effective field of the I spins $(\mathbf{H}_{\text{eff}})_I$ is then[14]

$$(\mathbf{H}_{\text{eff}})_I=\mathbf{i}(H_1)_I+\mathbf{k}h_0, \tag{3}$$

where $\mathbf{i}$ and $\mathbf{k}$ are unit vectors along the directions of $(H_1)_I$ and H_0, respectively. Since $h_0 \gg (H_1)_I$, $\mathbf{M}_I$ is essentially parallel to $(\mathbf{H}_{\text{eff}})_I$.

h_0 is now slowly decreased to zero. By slowly, we mean taking a time of about 30 msec, which is quite long compared to the precession period of the I spins in the field $(H_1)_I$. During such a slow variation $\mathbf{M}_I$ remains parallel to $(\mathbf{H}_{\text{eff}})_I$, so that when h_0 has returned to zero $\mathbf{M}_I$ is parallel to $(H_1)_I$. If $(H_1)_I$ is large compared to a magnetic field H_L which we call the "local field" and shall define in Sec. III, we shall see that $\mathbf{M}_I$ will be equal to the thermal equilibrium value $(M_I)_0$ given by the relation

$$\begin{aligned}(M_I)_0&=\frac{N_I\gamma_I^2\hbar^2 I(I+1)}{3k\theta_L}H_0\\ &=C_I H_0/\theta_L,\end{aligned} \tag{4}$$

where N_I is the number of I spins per unit volume, θ_L is the lattice temperature, k is Boltzmann's constant, and C_I is the Curie constant of the I spins.

If $(H_1)_I$ is comparable to or less than H_L, $\mathbf{M}_I$ is less than $(M_I)_0$, as shown in Ref. 10. However, the decrease below $(M_I)_0$ is a reversible one. Moreover, no further decrease will take place except via the slow spin-lattice coupling. This relaxation time, Redfield's T_{2e}, is much longer than $(T_2)_I$, being in fact 30 sec for Li^7 at 1.5°K.

As has been emphasized in Ref. 10, the technique of bringing $\mathbf{M}_I$ parallel to $(H_1)_I$ may be thought of as an adiabatic demagnetization in the I spin rotating reference frame.

We are now ready to turn on the second rotating field $(H_1)_S$. This we do, holding it on for a time t_{on}. Since $(H_1)_S$ is turned on quickly compared to the precession period of $\mathbf{M}_S$ about $(H_1)_S$, and since $H_0=H_{00}$, $\mathbf{M}_S$ is perpendicular to $(H_1)_S$. It remains so, precessing about $(H_1)_S$ in the rotating frame, and decaying to zero in a time $(T_2)_S$, typically a few hundred microseconds.[10] The S spins are now at an infinite spin temperature in their rotating reference frame. By means of the dipolar coupling between the I and S spins, the entire system of I and S spins now comes to a common spin temperature. This involves a decrease in $\mathbf{M}_I$ since the I spins have been heated by their contact with the S spins. By the same token, the S spins have been cooled. They, therefore, acquire magnetization parallel to their effective field, hence, along $(H_1)_S$. After the time t_{on}, $(H_1)_S$ is turned abruptly to zero. In the absence of $(H_1)_S$, $\mathbf{M}_S$ decays to zero in the time $(T_2)_S$.[10] As we shall see, nothing happens to the I magnetization during this decay. After a time t_{off}, $(H_1)_S$ is once again turned on, the whole cycle being repeated until it has been performed N times.

Following the Nth cycle, we wish to observe the extent that $\mathbf{M}_I$ has been diminished. Accordingly, $(H_1)_I$ is switched abruptly to zero, and the free induction decay of the I spins is observed photographically on an oscilloscope. The amplitude of the induction decay immediately after the turn-off of $(H_1)_I$ is a measure of $\mathbf{M}_I$.

The experimental technique described above differs in two ways from that of Hahn and Hartmann. The first difference is the manner in which $\mathbf{M}_I$ is brought

[12] B. N. Provotorov, Zh. Eksperim. i Teor. Fiz. **41**, 1582 (1961) [translation: Soviet Phys.—JETP **14**, 1126 (1962)]; and A. G. Redfield, Phys. Rev. **128**, 2251 (1962).
[13] A. G. Redfield, Phys. Rev. **130**, 589 (1963).
[14] See, for example, C. P. Slichter, in *Principles of Magnetic Resonance* (Harper and Row Publishers, New York, 1963).

parallel to $(H_1)_I$. Hahn and Hartmann apply a 90° pulse. This puts $\mathbf{M}_I$ perpendicular to both $(H_1)_I$ and H_0. In order to get $\mathbf{M}_I$ along $(H_1)_I$, they then shift the phase of $(H_1)_I$ by 90°.

The second difference in their technique involves the other alternating field $(H_1)_S$. Instead of pulsing it off and on, they turn it on at fixed amplitude, but periodically shift its phase by 180°. They do this at a rate sufficiently fast compared to the cross-relaxation time between the S and I spins so that the S spins are unable to achieve magnetization parallel to $(H_1)_S$. In this manner they hold the S spins at an effectively infinite temperature. This technique, though experimentally somewhat more involved than simply turning $(H_1)_S$ on and off, has the advantage of giving the maximum rate of heating. As we have remarked, their theoretical analysis is analogous to that of the flow of heat to an object via a rod connected to a reservoir of fixed temperature. (Of course, holding the S spins at a fixed spin temperature is not an *essential* feature of Hahn and Hartmann's method. However, the bulk of their theoretical analysis using the density matrix is based on this assumption.)

III. THEORETICAL ANALYSIS

A. Basic Equations

In this section, we derive the basic theoretical expressions needed to analyze our experiment. We start by writing the Hamiltonian of the system in the laboratory frame.

$$\mathcal{H}=\mathcal{H}_{ZI}(t)+\mathcal{H}_{ZS}(t)+(\mathcal{H}_d)_{II}+(\mathcal{H}_d)_{SS}+(\mathcal{H}_d)_{IS}, \quad (5)$$

where $\mathcal{H}_{ZI}(t)$ is the Zeeman energy of the I spins. It includes both a static interaction with field $H_0\mathbf{k}$ and a time-dependent interaction to the two alternating fields. It is most convenient to consider that rotating fields have been applied, instead of linearly polarized alternating fields. We have, then

$$\mathcal{H}_{ZI}(t)=-\gamma_I\hbar\mathbf{I}\cdot[\mathbf{k}H_0+\mathbf{i}(H_1)_I\cos\Omega_I t+\mathbf{j}(H_1)_I\sin\Omega_I t +\mathbf{i}(H_1)_S\cos\Omega_S t+\mathbf{j}(H_1)_S\sin\Omega_S t], \quad (6)$$

where Ω_I and Ω_S may be positive or negative, to represent either sense of rotation, and where

$$\mathbf{I}=\sum_j \mathbf{I}_j \quad (6a)$$

is the total spin vector of the I spins.

The terms $(\mathcal{H}_d)_{IS}$, etc., represent the magnetic dipolar coupling of the I spins with the S spins, and so forth.

We now wish to transform to a rotating reference system. In so doing, we are following Redfield.[4] However, our problem is somewhat different from his since we have two rotating fields. We therefore wish to transform in such a way that we view the I spins and S spins in their respective reference frames. This is readily accomplished[14] by introducing the unitary operator T defined as

$$T=\exp(i\Omega_I I_z t)\exp(i\Omega_S S_z t), \quad (7)$$

where

$$I_z=\sum_j I_{zj}, \qquad S_z=\sum_k S_{zk}, \quad (8)$$

are the total z components of angular momentum of the two spin species.

We define a new wave function Ψ' by the equation

$$\Psi'=T\Psi. \quad (9a)$$

Then substituting $T\Psi'$ for Ψ, Schrödinger's equation becomes

$$\frac{\hbar}{i}\frac{\partial\Psi'}{\partial t}=\mathcal{H}'\Psi', \quad (9b)$$

where $\mathcal{H}'$ is a transformed Hamiltonian.

Explicit evaluation of $\mathcal{H}'$ using standard techniques[14] gives

$$\mathcal{H}'=-\gamma_I\hbar[(H_0+\Omega_I/\gamma_I)Iz+(H_1)_I I_x] -\gamma_S\hbar[H_0+\Omega_S/\gamma_S)Sz+(H_1)_S S_x] +\mathcal{H}_{dII}{}^0+\mathcal{H}_{dIS}{}^0+\mathcal{H}_{dSS}{}^0 +\text{time-dependent terms we ignore.} \quad (10)$$

The terms $\mathcal{H}_{dII}{}^0$, etc., represent that part of the dipolar coupling $\mathcal{H}_{dII}$ that commutes with the Zeeman interaction between the spins and the static laboratory field, H_0. These terms are usually called the "secular part" of the dipolar interaction. We write them out explicitly below.

The time-dependent terms are of two sorts. One variety arises from the nonsecular parts of the dipolar coupling. They oscillate at frequencies Ω_I, Ω_S, or $(\Omega_I\pm\Omega_S)$. The second sort arises from couplings of the I spins to $(H_1)_S$ and the S spins to $(H_1)_I$. These oscillate at a frequency $(\Omega_I-\Omega_S)$. Since Ω_I, Ω_S, and $(\Omega_I\pm\Omega_S)$ are all far from any of the energy level spacings in the rotating frame, they can be neglected. One must remember, however, that it is conceivable that should there be a quadrupolar interaction added, and should the two nuclei have similar γ's (as do, for example, Cu^{63} and Cu^{65}), the frequency $(\Omega_I-\Omega_S)$ might, in fact, be close to a possible transition.

If one chooses

$$\Omega_I=-\gamma_I H_{00}, \qquad \Omega_S=-\gamma_S H_{00}, \quad (11)$$

the two nuclei are exactly at resonance. Note that the two Ω's are negative if the γ's are positive, representing the fact that nuclei of positive γ rotate in the "negative" sense about H_0. Making use of Eq. (11), recalling that $H_0-H_{00}=h_0$, and neglecting the time-dependent terms

of $\mathcal{H}'$, we have

$$\mathcal{H}'=-\gamma_I\hbar[h_0I_z+(H_1)_II_x]-\gamma_S\hbar[h_0S_z+(H_1)_SS_x]+\mathcal{H}_{dII}{}^0+\mathcal{H}_{dIS}{}^0+\mathcal{H}_{dSS}{}^0. \quad (12)$$

It is convenient to define the Zeeman energies $\mathcal{H}_{ZI}$ and $\mathcal{H}_{ZS}$ by the equations

$$\mathcal{H}_{ZI}=-\gamma_I\hbar[h_0I_z+(H_1)_II_x], \text{ etc.} \quad (13)$$

The dipolar terms are

$$\mathcal{H}_{dII}{}^0=\frac{\gamma_I{}^2\hbar^2}{4}\sum_{j,k}(3I_{zj}I_{zk}-\mathbf{I}_j\cdot\mathbf{I}_k)\frac{1-3\cos^2\theta_{jk}}{r_{jk}{}^3}$$

$$\mathcal{H}_{dIS}{}^0=\gamma_I\gamma_S\hbar^2\sum_{k,p}I_{zk}I_{zp}\frac{(1-3\cos^2\theta_{kp})}{r_{kp}{}^3} \quad (14)$$

and similarly for $\mathcal{H}_{dSS}{}^0$. To these may be added the pseudodipolar and pseudoexchange couplings where their size is large enough to be important.

It is the term $\mathcal{H}_{dIS}{}^0$ which gives rise to the effects observed by Bloembergen and Sorokin[6] in their studies of CsBr. They found that the rapid bromine spin-lattice relaxation could communicate itself to the Cs nuclei through this term when the Cs nuclei were quantized along their own H_1.

We can view the various terms of Eq. (12) as energy reservoirs of Zeeman or dipolar energy. Since the various terms do not commute, they can exchange energy. Such processes may be termed cross relaxation in the double-rotating reference frame. The rate of cross relaxation will depend on how the energy levels of the different terms match, on the heat capacities, and on the strength of coupling as measured by the failure of terms to commute with one another. Thus, we note that the Zeeman term of the I spins $\mathcal{H}_{ZI}$ commutes with the Zeeman energy of the S spins, $\mathcal{H}_{ZS}$. However, as long as $(H_1)_I\neq 0$, $\mathcal{H}_{ZI}$ does not commute with either $\mathcal{H}_{dII}{}^0$ or $\mathcal{H}_{dIS}{}^0$. We can, therefore, transfer energy between $\mathcal{H}_{ZI}$ and $\mathcal{H}_{dII}{}^0$ or $\mathcal{H}_{dIS}{}^0$. Moreover, $\mathcal{H}_{dIS}{}^0$ provides a coupling mechanism to transfer energy between $\mathcal{H}_{ZI}$ and $\mathcal{H}_{ZS}$ [provided $(H_1)_S\neq 0$].

All these remarks lead one, following Redfield, to assume that if one waits long enough, the various parts of Eq. (12) will come to an equilibrium in which the system can be described by a common temperature θ. For some purposes, it may also be possible and convenient to assume that various parts may come to common temperatures faster than the whole system achieves a single temperature. This is the viewpoint we adopt in the Appendix to calculate some cross-relaxation times.

We, therefore, make the assumption that when the system has achieved a common temperature it is described by a density matrix ρ given as

$$\rho=\frac{\exp(-\mathcal{H}'/k\theta)}{\mathrm{Tr}\exp(-\mathcal{H}'/k\theta)}, \quad (15)$$

where $\mathcal{H}'$ is given by Eq. (12). In terms of ρ we can calculate the average energy E and the average magnetization vector $\langle\mathbf{M}_I\rangle$ in the high temperature approximation

$$E=\mathrm{Tr}(\rho\mathcal{H}')=-\frac{C_I[(H_1)_I{}^2+h_0{}^2+H_L{}^2]+C_S[(H_1)_S{}^2+h_0{}^2]}{\theta}, \quad (16a)$$

$$\langle\mathbf{M}_I\rangle=\mathrm{Tr}(\rho\gamma_I\hbar\mathbf{I})=\frac{C_I(\mathbf{H}_{\mathrm{eff}})_I}{\theta}, \quad (16b)$$

where C_I and C_S are the Curie constants given in terms of the number of I or S spins per unit volume, N_I or N_S and Boltzmann's constant k by

$$C_I=\frac{\gamma_I{}^2\hbar^2I(I+1)N_I}{3k}, \text{ etc.,} \quad (17)$$

and where $H_L{}^2$ is defined by the equation

$$\frac{C_IH_L{}^2}{\theta}=\mathrm{Tr}\rho(\mathcal{H}_{dII}{}^0+\mathcal{H}_{dIS}{}^0+\mathcal{H}_{dSS}{}^0). \quad (18)$$

Evaluating the trace gives

$$H_L{}^2=\tfrac{1}{3}\langle\Delta^2H\rangle_{II}+\langle\Delta^2H\rangle_{IS}+\frac{1}{3}\frac{\gamma_S{}^2N_SS(S+1)}{\gamma_I{}^2N_II(I+1)}\langle\Delta^2H\rangle_{SS}, \quad (19)$$

where $\langle\Delta^2H\rangle_{\alpha\beta}$ is the contribution (in gauss) of the β spins to the second moment of the α-spin resonance line. (Incorrect expressions for $H_L{}^2$ have been given in both Refs. 4 and 10.) H_L has the dimensions of a magnetic field. Although we call it the "local field," it should not be confused with the Lorentz local field. Actually, H_L is introduced simply to enable us to factor C_I out of various equations. The fact that the dipolar energy is $[-C_IH_L{}^2/\theta]$ makes it appear superficially that we have taken into account only the I spins in calculating the dipolar energy. However, that such is not the case is seen by examining Eqs. (18) and (19) which exhibit explicitly the dipolar contribution of the S species to the expression for H_L. $C_IH_L{}^2$ measures the total dipolar contribution to the spin specific heat. Note that although the term "local field" sounds vague, that H_L can in fact be calculated *exactly* and is to be considered throughout as a precisely predicted quantity. The only exception to this statement is found when pseudodipolar coupling becomes prominent as in higher atomic number elements.

It is $\langle\mathbf{M}_I\rangle$ which we observe from our oscilloscope photographs of the initial height of the free induction decay following turn-off of $(H_1)_I$.

One further expression is needed. It is the expression obtained from Ref. 10, for the magnetization $\mathbf{M}_I$ found after the demagnetization of I's. That is, suppose $(H_1)_S=(H_1)_I=0$, and that $\mathbf{M}_I=\mathbf{k}M_{I0}$ where

$$M_{I0}=C_I H_0/\theta_L \tag{20}$$

is the thermal equilibrium magnetization of the I spins at the lattice temperature θ_L. With $h_0 \gg H_L$, we switch on $(H_1)_I$, and slowly reduce h_0 to zero. We then end up, according to Eq. (16), with

$$\langle \mathbf{M}_I \rangle = \mathbf{i} M_{I0} \frac{(H_1)_I}{[(H_1)_I^2+H_L^2]^{1/2}}. \tag{21}$$

Note that if we were to change $(H_1)_I$ slowly, $\langle \mathbf{M}_I \rangle$ would follow $(H_1)_I$ in accord with Eq. (21).

B. Analysis of the Experimental Procedure

We now turn to an analysis of our experiment. We shall assume throughout that spin-lattice relaxation can be neglected during the times of the experiment. Spin-lattice processes can be included readily, but one must be careful in so doing to include the sort of transverse Overhauser effects described by Bloembergen and Sorokin.[6]

We begin by the demagnetization process. This brings $\langle \mathbf{M}_I \rangle$ down along the x axis, its magnitude being given by Eq. (21). Let us call this magnetization $(\mathbf{M}_I)_i$. During this process, since $(H_1)_S$ is zero, $\mathcal{H}_{ZS}$ commutes exactly with the rest of the Hamiltonian. So, likewise, does $\gamma_S \hbar S_z$. Therefore, $\langle \mathbf{M}_S \rangle$ remains unaffected, and points along the static laboratory field $\mathbf{H}_0$. The rest of $\mathcal{H}'$ is at a common temperature θ_i which we can compute from Eqs. (16b) and (21).

$$\theta_i = C_I (H_1)_I/(M_I)_i. \tag{22}$$

This temperature is, of course, very much lower than the lattice temperature θ_L.

We now turn on $(H_1)_S$ suddenly. In such a rapid process, the state of the system does not change. The dipolar energy and the Zeeman energy of the I spins are therefore unchanged. The S-spin Zeeman energy E_S

$$E_S = -\langle \mathbf{M}_S \rangle \cdot (\mathbf{H}_{\text{eff}})_S, \tag{23}$$
$$= 0$$

since $\langle \mathbf{M}_S \rangle$ and $(\mathbf{H}_{\text{eff}})_S$ are perpendicular. The total energy of the system E_i is therefore

$$E_i = -\frac{C_I[(H_1)_I^2+H_L^2]}{\theta_i}. \tag{24}$$

After a sufficiently long time, the S-spins Zeeman energy comes into thermal equilibrium with the rest of the system at a common final temperature θ_f. The final energy E_f is then

$$E_f = -\frac{C_I[(H_1)_I^2+H_L^2]+C_S(H_1)_S^2}{\theta_f}. \tag{25}$$

But since the total system is isolated and its Hamiltonian independent of time, its energy cannot change. Therefore,

$$E_i = E_f. \tag{26}$$

This gives us that

$$\frac{\theta_i}{\theta_f} = \frac{C_I[(H_1)_I^2+H_L^2]}{C_I[(H_1)_I^2+H_L^2]+C_S(H_1)_S^2} \tag{27}$$
$$= \frac{1}{1+\epsilon},$$

where

$$\epsilon \equiv \frac{C_S(H_1)_S^2}{C_I[(H_1)_I^2+H_L^2]}. \tag{28}$$

In the process the magnitude of $\langle \mathbf{M}_I \rangle$ drops from its initial value $(M_I)_i$ to a final value $(M_I)_f$ which, in view of Curie's law, is

$$(M_I)_f/(M_I)_i = 1/(1+\epsilon). \tag{29}$$

We now suddenly turn off $(H_1)_S$. Once again the system immediately after the change has the same wave function as it did just before. The expectation value of $\mathcal{H}_{ZI}$ and of the dipolar energies is thus unchanged, but that of $\mathcal{H}_{ZS}$ is zero since $(H_{\text{eff}})_S=0$. The total energy E_f' is therefore

$$E_f' = -\frac{C_I[(H_1)_I^2+H_L^2]}{\theta_f}. \tag{30}$$

Immediately after the turn-off of $(H_1)_S$, $\langle \mathbf{M}_S \rangle$ is nonzero. Therefore, we see that we do not have thermal equilibrium. If we wait for a sufficiently long time, the entire system will come to a common temperature θ_{ff}. In the process, $\langle \mathbf{M}_S \rangle$ decays to zero. This is an irreversible decay. We shall in fact calculate the entropy increase below.

When the system has reached the final temperature θ_{ff}, the energy is E_{ff}. Using Eq. (16a) we have

$$E_{ff} = -C_I[(H_1)_I^2+H_L^2]/\theta_{ff}. \tag{31}$$

But $E_{ff}=E_f'$ since the spin system is isolated from the outside world and has a Hamiltonian independent of time. Therefore, using Eqs. (30) and (31)

$$\theta_f = \theta_{ff}. \tag{32}$$

Using Curie's law we see that following the turn-off of $(H_1)_S$, $\langle \mathbf{M}_I \rangle$ does not change.

For one complete on-off cycle, therefore, we can argue that $\langle \mathbf{M}_I \rangle$ is reduced by the factor $1/(1+\epsilon)$.

We can repeat the argument for another on-off cycle.

The magnetization $M_I(N)$ after N cycles is thus given in terms of its value $M_I(0)$ prior to the first cycle by

$$M_I(N)/M_I(0)=[1/(1+\epsilon)]^N. \tag{33}$$

When $\epsilon \ll 1$, as in our experiments, we can write this as

$$M_I(N)/M_I(0)=e^{-N\epsilon}, \tag{34}$$

where ϵ is given by Eq. (28). Equation (34) is our principal theoretical result and its verification, the chief objective of our experiments, is discussed in Sec. V.

As pointed out in Sec. I, double resonance is possible even when $(H_1)_I \ll H_L$. Experimentally we accomplish this by performing adiabatic reduction of (H_1) after M_I has been brought along $(H_1)_I$ in the rotating frame. After $(H_1)_I \simeq 0$, $M_I \simeq 0$ from Curie's law, however, we have retained the order in the I-spin system, the order now being with respect to the local field.[10] $(H_1)_S$ is now cycled on and off N times. After the Nth cycle, $(H_1)_I$ is adiabatically returned to its original value. The resulting M_I is then observed by rapidly turning off $(H_1)_I$ and observing the free induction decay.

The analysis for the case when $(H_1)_I \ll H_L$ is essentially the same as given above; however, now, the term $C_I(H_1)_I^2/\theta$ no longer appears in Eqs. (24) and (25), and ϵ reduces to

$$\epsilon=C_S(H_1)_S^2/C_I H_L^2.$$

C. Energy and Entropy

It is interesting to follow the changes in energy and entropy of the spins that take place during the double resonance. The essence of the experiment is the heating of the I spins brought about by the contact with the hot S spins. There is a net flow of energy into the system as a result of work done on the S spins. The destruction of the I magnetization corresponds to an irreversible loss of order, that is, an entropy increase. The energy of the system is, of course, the expectation value of the Hamiltonian of Eq. (12). Basic theorems of quantum (and classical) mechanics tell us that the total energy remains constant as long as $\mathcal{H}$ does not explicitly depend on time. Rearrangements of energy within the total system even when $\mathcal{H}$ is independent of time we identify as a heat flow within the system. Changes of the total energy due to variation of an external parameter we call work on or by the spin system.

We can follow the cycle by considering work and heat transfer in the rotating frame. Consider one complete cycle of $(H_1)_S$ on and off. We start by turning on $(H_1)_S$ suddenly. Bearing in mind that the S Zeeman energy is

$$\langle \mathcal{H}_{ZS} \rangle = -\langle \mathbf{M}_S \rangle \cdot (\mathbf{H}_1)_S, \tag{35}$$

and that during the sudden turn-on the dipolar energy does not have time to change, we see that it takes no work to turn on $(H_1)_S$ since $\langle \mathbf{M}_S \rangle$ is initially zero. The establishment of the S magnetization causes $\langle \mathcal{H}_{ZS} \rangle$ to go from zero to a negative value. That is, there is a heat flow from the S-spin Zeeman reservoir to the rest of the spin system. That this is the direction of heat flow is reasonable since the initial zero $\langle \mathbf{M}_S \rangle$ in the presence of a nonzero $(H_1)_S$ can be viewed as saying that $\mathcal{H}_{ZS}$ has an infinite temperature. Associated with this heat flow between systems at different temperature there must be an entropy increase.

Following establishment of $\langle \mathbf{M}_S \rangle$, we turn off $(H_1)_S$. Using Eq. (35) we can see that we must do positive work on $\mathcal{H}_{ZS}$ in the process. [Note that during turn-on or turn-off, which takes place suddenly, there is no time for heat flow, so that we can compute the work done solely from the changes in $\langle \mathcal{H}_{ZS} \rangle$ given by Eq. (35).] Following turn-off, $\langle \mathbf{M}_S \rangle$ decays irreversibly to zero. Again there must be an entropy increase associated with the irreversibility. We are now ready to repeat the cycle. Note that we have done a net amount of work on the spin system, and that there has been an irreversible loss in order.

Had we turned on $(H_1)_S$ in the next cycle *before* $\langle \mathbf{M}_S \rangle$ had been able to decay, the S spins would have done positive work back on us. In fact, had $\langle \mathbf{M}_S \rangle$ not decayed at all, we would have gotten back as much work as we put in when we turned off $(H_1)_S$. We would not then have done any net work in a cycle. Moreover, apart from the effects at the original turn-on, there would have been no irreversible loss in magnetization of either spin system. We must allow a sufficiently long time for the irreversible features to occur.

The entropy σ of the system, can be calculated starting from the basic equation[15]

$$\sigma=\frac{E+k\theta \ln Z}{\theta}, \tag{36}$$

where Z is the partition function. Making use of the high-temperature approximation, we can evaluate Eq. (36) to get

$$\sigma \cong k\left[\ln(\mathrm{Tr}1)-\frac{1}{2k^2\theta^2}\frac{\mathrm{Tr}\mathcal{H}^2}{\mathrm{Tr}1}\right], \tag{37}$$

where Tr1 means the total number of states, and equals

$$\mathrm{Tr}1=(2I+1)^{N_I}(2S+1)^{N_S}. \tag{38}$$

Evaluating $\mathrm{Tr}\mathcal{H}^2$, as in Eq. (16a), gives (with $h_0=0$)

$$\sigma=k[N_I \ln(2I+1)+N_S \ln(2S+1)] - \frac{C_I[(H_1)_I^2+H_L^2]+C_S(H_1)_S^2}{2\theta^2}. \tag{39}$$

[Note that Eq. (21), describing the adiabatic demagnetization, follows from use of Eq. (16b), Curie's

[15] R. C. Tolman, in *Principles of Statistical Mechanics* (Oxford University Press, Oxford, 1938).

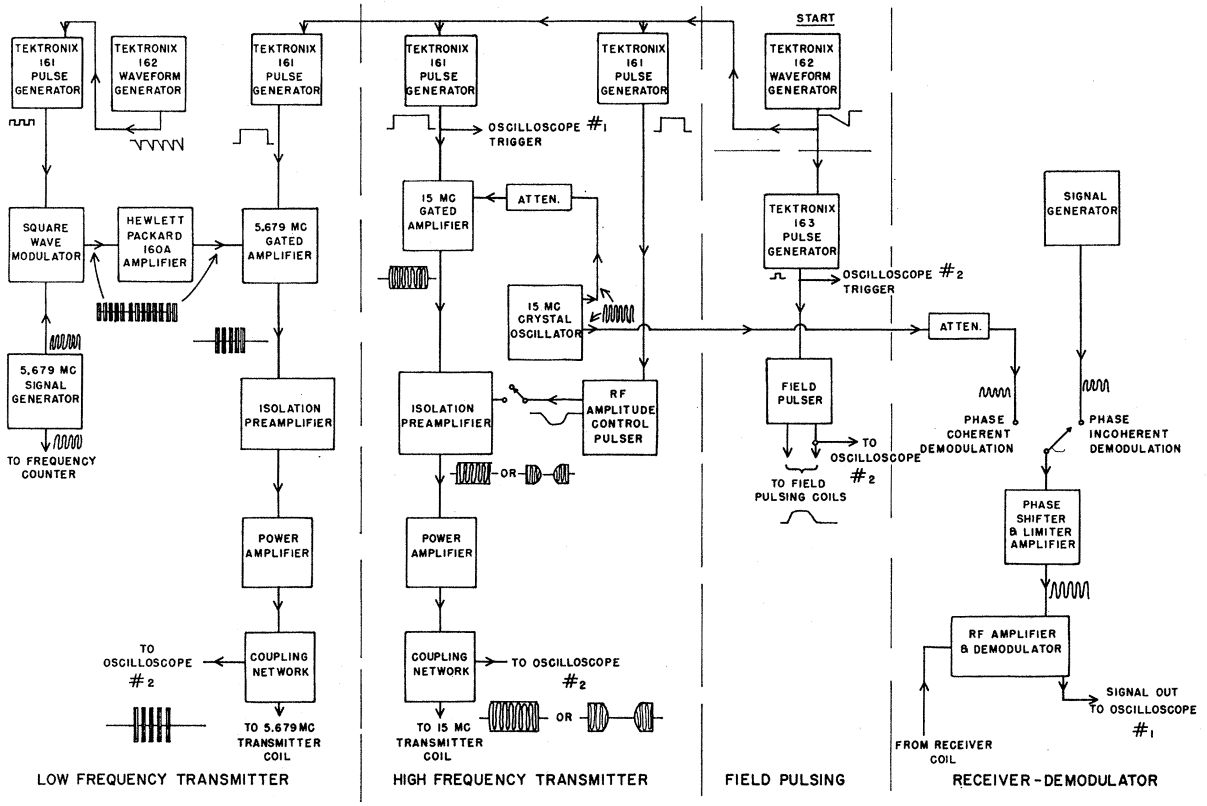

FIG 1. Block diagram of the double resonance apparatus.

law, together with the requirement that the entropy given by Eq. (39) remain constant.] Since we have worked out the temperature at each part of the cycle, we can use Eq. (39), together with the approximation that ϵ is small, to find that in one complete cycle starting at temperature θ there is a total increase in entropy $\sigma_f-\sigma_i$ of

$$\sigma_f-\sigma_i=\frac{C_S(H_1)_S^2}{\theta^2}. \tag{40}$$

Half of the increase occurs following the turn-on, the other half following the turn-off of $(H_1)_S$. We note that the larger $(H_1)_S$, the larger the change of entropy per cycle. Since the existence of $\mathbf{M}_I$ is a sign of order, we see that a large $(H_1)_S$ leads to a large destruction of $\mathbf{M}_I$, as was, in fact, already expressed by Eq. (34).

IV. EXPERIMENTAL DETAILS

A. Apparatus

The experiment was performed using the pulsed double resonance spectrometer shown in block diagram form in Fig. 1. The rf head was a miniature crossed-coil configuration which fit inside a set of liquid helium dewars. The coil configuration is shown in Fig. 2. Most of the data taken in the experiment were at 1.5°K. The individual components of the spectrometer are of standard design and are described in detail elsewhere.[16] However, a few features of the apparatus which were useful for the present experiment will be described.

The two transmitter coils were tuned to 15.00 and 5.679 Mc/sec, respectively, the resonant frequencies of the Li^7 and Li^6 nuclei in a field of 9062 G. The coupling between the final power amplifiers and the transmitter tank circuits was accomplished by a link, the input end of which was the "pi section" output network of the power stage. The rf voltage, and thus the H_1 field, were varied in magnitude by changing the loading capacitor which formed the final leg of the "pi section." This arrangement provided a simple means of varying the H_1 fields and had very little effect on the tuned circuits. The rf voltages were monitored on an oscilloscope by means of capacitive dividers across the transmitter tank circuits.

In experiments in the completely demagnetized state, $(H_1)_7 \ll H_L$, the $(H_1)_7$ field was reduced to a small value by pulsing the grid bias of the preamplifier which drives the final power stage. This reduced the $(H_1)_7$ field to a few milligauss, and since $H_L=1.2$ G in metallic lithium, the criterion that $(H_1)_7 \ll H_L$ was well satisfied.

The receiver coil was tuned to 15.00 Mc/sec and connected directly to the grid of the input stage of the

[16] F. M. Lurie, thesis, University of Illinois, 1963 (unpublished).

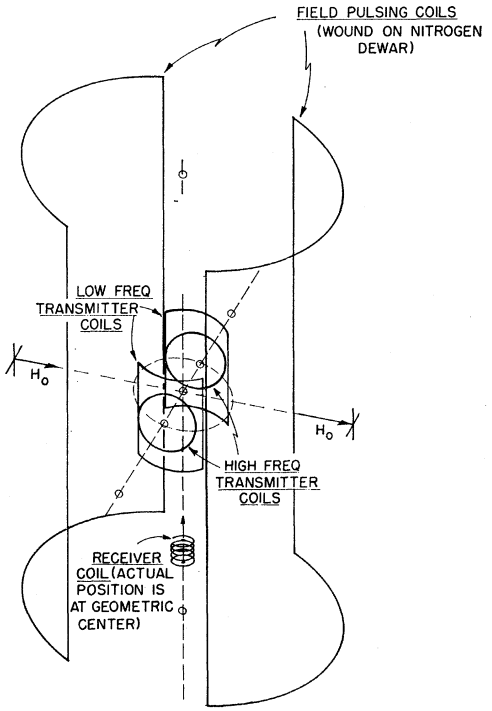

FIG. 2. Schematic diagram of the coil geometry at the sample.

receiver. The receiver had a gain of 10^4 and was linear over the range of signals encountered. Since signal to noise was not a problem at 1.5°K, a box-car integrator was not needed, so that phase incoherent detection was used. The free induction decay of the Li^7 nuclei was observed photographically on an oscilloscope which was dc coupled to the detector and triggered by the turn-off of the $(H_1)_7$ pulse. In order to achieve a linear detection, an rf reference of several volts amplitude but differing slightly in frequency from the 15.00 Mc/sec was fed to the detector. The oscilloscope photographs therefore show the beat between the reference and the signal. Use of a reference which is incoherent with the signal makes the instrumental adjustments substantially simpler than they are when a phase coherent reference is employed, yet preserves the enormous advantage of linearity of the detection process which is only possible when the signal voltage is small compared to the reference.

B. Calibration of the H_1 Fields

In order to test the thermodynamic theory presented in the previous section, the magnitudes of the H_1 fields must be accurately known. In particular, this required field calibrations at room temperature, 78°K, and 1.5°K and at the frequencies used during the experiment. At room temperature and 1.5°K, calibrations were made by applying a 180° pulse, or $n\pi$ pulse where n is an integer, to a narrow resonance line and detecting the null in the free induction decay. A narrow line, i.e., $\delta H \ll H_1$, is required for precision in the H_1 calibration. At room temperature the 15-Mc/sec field was calibrated using the motionally narrowed[5] resonance of Li^7 nuclei in the metal particles and the protons in the mineral oil surrounding the lithium particles. The 5.679-Mc/sec field was calibrated on the protons in the mineral oil. At 1.5°K the 180° pulse method was used on both transmitter coils with a small quantity of liquid He^3 which was introduced into the center of the lithium sample. These calibrations showed that the field calibrations were essentially independent of temperature and all calibration runs gave the same results to within 3%. In addition, some of the calibrations were performed with the second field being pulsed on. No detectable effect due to the second rf field was found.

The homogeneity of the H_1 fields is believed to be fairly good. Inhomogeneity in the H_1's can arise from two causes (a) effects due to the coil geometry and (b) the existence of the skin effect in the metal particles. A rough estimate of the geometrical effect over the sample volume could be made from the calibration data on the liquid He^3. This indicated that the H_1 field at one end of the receiver coil was nine-tenths the value at the center. Since the lithium sample length was less than one-half the receiver coil length, the actual variation of H_1 over the Li samples was probably much smaller than the above estimate. Further evidence for this is that no indications of H_1 inhomogeneities were observed in the calibrations using Li^7 and protons at room temperature. Therefore, we conclude that spatial H_1 variations were small and probably negligible compared to skin depth effects which are discussed below. We discuss the broadening of H_1 due to the skin effect in Sec. B below.

The 15-Mc/sec field was also calibrated using the Li^7 nuclei at 78°K and 1.5°K by means of the adiabatic demagnetization process described in the previous section. The procedure was to pulse the static field off resonance, turn on the $(H_1)_7$ at the peak of the field pulse, and then return the static field adiabatically to the resonance value. $(H_1)_7$ is then pulsed off and the free induction decay photographed. This process is repeated for successively smaller values of $(H_1)_7$. If the resulting Li^7 magnetization is plotted as a function of $(H_1)_7$, the experimental points should fall on a curve given by Eq. (21),

$$M_7 = M_0(H_1)_7/[H_L^2+(H_1)_7^2]^{1/2}.$$

Since H_L can be calculated theoretically, a curve given by Eq. (21) is a calibration of $(H_1)_7$ provided M_0 is known. At the $M_7=0.707M_0$ point, $(H_1)_7=H_L$ which calibrates $(H_1)_7$ in terms of the voltage across the transmitter tank circuit which corresponds to H_L. A typical result for this type of calibration at 78°K is shown in Fig. 3. The solid curve is calculated from Eq. (21). Its horizontal scale is given by the theoretical H_L (1.20 G) and the calibration of $(H_1)_7$ by the 180°

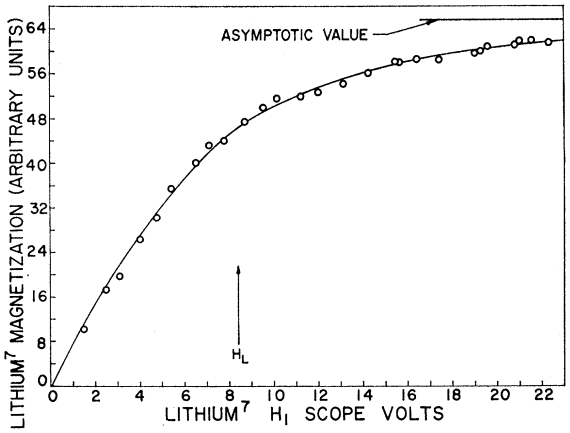

FIG. 3. Li^7 magnetization as a function of $(H_1)_7$ (in volts) for an adiabatic demagnetization in the rotating reference frame at 78°K. The solid curve is calculated from Eq. (21). The horizontal scale is determined by the theoretical value of H_L (1.20 G) and the calibration of $(H_1)_7$ in terms of voltage by the 180° pulse method. The vertical scale was chosen to fit the data at the value of $(H_1)_7=H_L$.

pulse. Its vertical scale is chosen to fit the data at the point $(H_1)_7=H_L$. The agreement between the calculated curve and the experimental points indicates that the two methods of calibration are consistent and provides a graphic demonstration of the adiabatic demagnetization process.

C. Samples

The lithium samples were composed of fine metal particles dispersed in mineral oil. The samples were made from 99.5% pure lithium ingot obtained from the Lithium Corporation of America. Pieces of the ingot were heated in mineral oil to 200°C, about 20°C above the melting point of lithium, and then agitated with a high-speed stirrer. The temperature was then lowered slowly with the stirrer running. All sample preparation was done under a dry helium atmosphere to reduce oxidation of the metal. Examination under a microscope revealed the metal particles to be generally spherical with an average radius of 3×10^{-3} cm. For pure metal, this radius is comparable to the classical skin depth at 78°K, and at 1.5°K the skin depth is undoubtedly much smaller than the particle size. However, for pure lithium at room temperature, the mean free path of electrons is about 100 Å. This is not greatly different from the contribution of the nearly 1% impurity, so that we do not expect the skin depth to vary greatly with temperature. There is good evidence that the rf fields were penetrating well into the lithium particles since the change in tuning of the receiver tank circuit was very small between room temperature and 1.5°K. We note, however, that the double resonance experiment involves two rf fields at different frequencies and, since the relative magnitudes of the field are important, our results are probably fairly sensitive to skin-depth effects. The experimental results to be presented in the next section do indicate that small skin-depth effects are present in our data. Resonance data indicating that these effects are indeed small will be described in the following section.

V. EXPERIMENTAL RESULTS

In this section the experimental results will be presented and compared with the thermodynamic theory developed in Sec. III. The experimental results will be compared with calculations using Eqs. (28) and (34) and the calibrated values of the H_1 fields. In the computations the value of H_L used will be the contribution from the interaction of Li^7 spins between themselves. The contributions to H_L from the terms involving the Li^6 spins are negligible being only about 2% of the total value of H_L. In this approximation we find the value of H_L^2 to be 1.43 G^2.[17]

A. Experiments with $(H_1)_7 \geq H_L$

The results described in this paragraph were all obtained at 1.5°K with $(H_1)_7$ about twice H_L. In Fig. 4 experimental values of $\ln M_7$ are plotted as a function of $(H_1)_6^2$ for $N=22$, $t_{on}=t_{off}=1$, 2, and 10 msec and $(H_1)_7=2.31$ G. For this value of $(H_1)_7$, $(H_1)_6=6.1$ G satisfies the Hahn condition. The solid line is calculated from Eqs. (28) and (34) and indicates the final value of the Li^7 magnetization corresponding to the establishment of a common spin temperature between the Li^7 and Li^6 spin systems. The results in Fig. 4 show that the two spin systems do achieve a common spin temperature over a range of values about the Hahn condition. Note that as the time during which mixing can occur is increased, the range of values of $(H_1)_6$ over

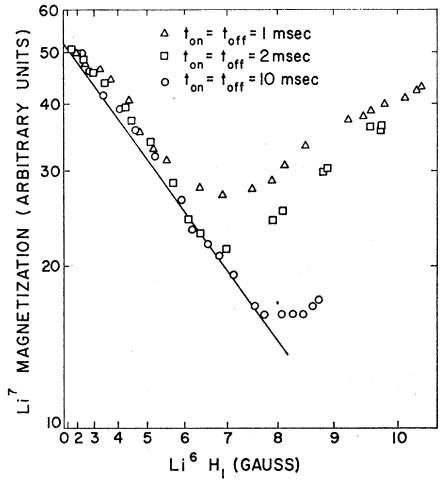

FIG. 4. $\ln M_7$ versus $(H_1)_6^2$ at 1.5°K for $N=22$, $t_{on}=t_{off}=1$, 2, and 10 msec, $(H_1)_7=2.31$ G. For this value of $(H_1)_7$, $(H_1)_6=6.1$ G satisfies the Hahn condition. The solid line is calculated from Eqs. (28) and (34)

[17] H. S. Gutowsky and B. R. McGarvey, J. Chem. Phys. **20**, 1472 (1952).

which a common spin temperature is reached increases as would be expected. Note also that there is a range of $(H_1)_6$ about the minimum in the curves over which the mixing is relatively insensitive to the value of $(H_1)_6$.

In Fig. 5 experimental values of $\ln M_7$ are plotted as a function of the number of mixing pulses N, with ϵ constant. These data were taken with $(H_1)_7=2.14$ G, $(H_1)_6=5.4$ G which approximately satisfy the Hahn condition. The solid line is again calculated from Eqs. (28) and (34) and agrees well with the data for the lower range of N. The deviation of the experimental points from a straight line for the large values of N is caused by skin effects as discussed in Sec. IV. (*Note added in proof.* The curvature may also result from the fact that H_L depends on the orientation of H_0 with respect to the crystal axes. Since the sample is a powder, a distribution

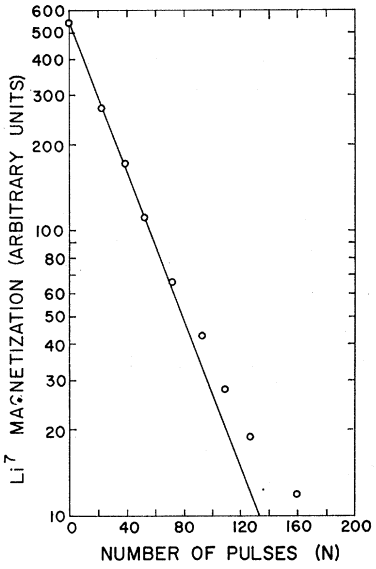

FIG. 5. $\ln M_7$ versus N at 1.5°K. $(H_1)_7=2.14$ G, $(H_1)_6=5.4$ G, nearly satisfying the Hahn condition. $t_{on}=t_{off}=4$ msec. The solid line is calculated using Eqs. (28) and (34).

in ϵ results.) Experimental evidence for this is given in Fig. 6 where the same kind of measurement was made, but with the $(H_1)_6$:$(H_1)_7$ ratio set to correspond to the region of the minima in the curves shown in Fig. 4. In this case the data should be less sensitive to small variations in the ratio of the H_1 fields. This is indeed indicated in Fig. 6 where only the last point deviates significantly from a straight line. In both Figs. 5 and 6 the data were taken with $t_{on}=t_{off}=4$ msec. Thus in these experiments more than 97% of the Li^7 magnetization has been destroyed in 1.25 sec in one case, and in 0.8 sec in the other.

B. Experiments with $(H_1)_7 \ll H_L$

In this paragraph results of experiments in the completely demagnetized state will be presented. All the data to be presented were obtained at 1.5°K and in this case Eqs. (28) and (34) apply with $(H_1)_7=0$. In

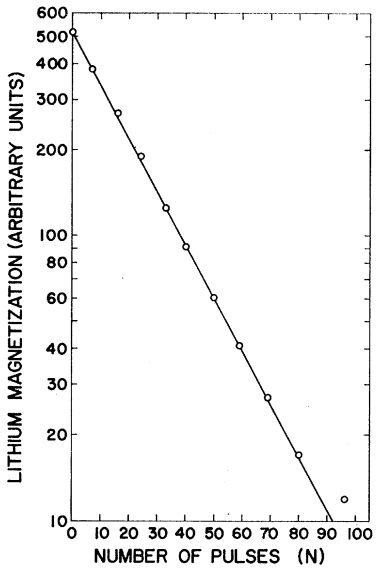

FIG. 6. $\ln M_7$ versus N at 1.5°K. $(H_1)_7=2.30$ G, $(H_1)_6=6.9$ G, $t_{on}=t_{off}=4$ msec. The ratio of $(H_1)_6$ to $(H_1)_7$ corresponds to the minimum in Fig. 4. The solid straight line is drawn to show the exponential dependence. This graph shows that the curvature in Fig. 5 results from slight inhomogeneities in the H_1's.

Fig. 7 $\ln M_7$ is plotted as a function of $(H_1)_6^2$ with $N=25$, and $t_{on}=t_{off}=2$, 5, and 8 msec. The solid line is calculated from Eqs. (28) and (34). In this case the data show that the rate of mixing decreases as $(H_1)_6$ is increased. This is a result of the competition between fast mixing at low $(H_1)_6$ and the increase in heat capacity for the Li^6 spin system for larger $(H_1)_6$. Notice that the curves have a very broad minimum which indicates that in the demagnetized state the setting of $(H_1)_6$ is not critical over a wide range. This fact could be of considerable importance in searching for an unknown resonance.

The results of an experiment in which $(H_1)_6$ is kept constant and N varied are shown in Fig. 8. In this case the data were taken with $(H_1)_6=6.4$ G and $t_{on}=t_{off}=6$ msec. This value of $(H_1)_6$ corresponds to a point in the

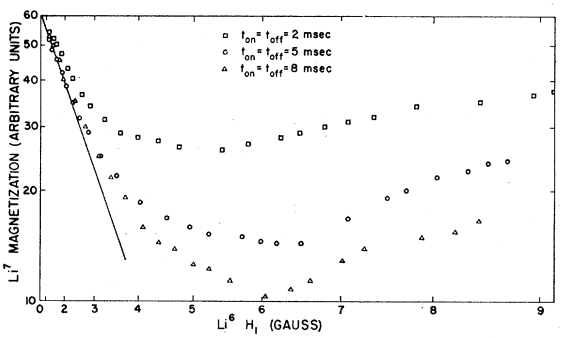

FIG. 7. $\ln M_7$ versus $(H_1)_6^2$ at 1.5°K for $N=25$, $(H_1)_7=0$, $t_{on}=t_{off}=2$, 5, and 8 msec. The solid line is calculated using Eqs. (28) and (34). This figure demonstrates that double resonance works in the completely demagnetized state. Note the broad minima.

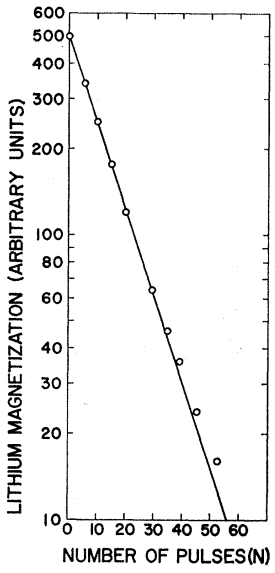

FIG. 8. $\ln M_7$ versus N at 1.5°K in the completely demagnetized state $[(H_1)_7=0]$. $(H_1)_6=6.4$ G, $t_{on}=t_{off}=6$ msec. The value of $(H_1)_6$ corresponds to the broad minimum in Fig. 7. The solid line is drawn to indicate the exponential dependence.

broad minimum of the curves in Fig. 7. In this case the solid line has been simply drawn through the data to indicate the exponential dependence. We do not have a theoretical value for its slope since we know that for this value of $(H_1)_6$ a common spin temperature is not established.

C. Discussion

The results presented in the previous paragraphs demonstrate the validity of the thermodynamic approach to the double resonance process. However, our data do not demonstrate fully the inherently attractive feature of the technique, namely, the increased sensitivity which is possible. We can obtain an estimate of the possible sensitivity from our data in the following way. In Figs. 5, 6, and 8 more than 95% of the Li^7 magnetization was destroyed in about one second. Since the Li^7 T_1 at 1.5°K is 30 sec, it would have been possible to take as long as 20 sec to destroy the Li^7 magnetization if this had been necessary. Roughly, this means that approximately 20 times fewer dilute spins could have been observed with the same signal to noise. Using the oscilloscope display, the signal to noise was good enough to permit one to gain another factor of 4 in the minimum detectable effect. A further increase in sensitivity could be achieved by employing gated integrator techniques and presenting the data on a chart recorder. On the other hand, as the number of dilute spins is decreased, the time required for mixing between the two spin systems may become limited by spin diffusion as has been pointed out by Hartmann and Hahn. Taking these factors into account, one estimates that approximately 10^{-5} dilute spins per abundant spin could be observed using the double resonance method without too great difficulty.

The data in Fig. 5 indicate that the double resonance technique can be used to determine the number of dilute spins in the material being studied. If the H_1 fields are calibrated and the nuclear spins and gyromagnetic ratios are known, the slope of a plot of $\ln M$ as a function of N, the number of mixing pulses, determines the ratio of the dilute to the abundant spins.

The good quantitative agreement between the data and theory not only demonstrates the validity of the thermodynamic approach to the double resonance process, but provides further justification of Redfield's hypothesis of a spin temperature in the rotating reference frame. In addition, the theory extends Redfield's ideas to the case of a common spin temperature in two reference frames simultaneously rotating at different frequencies, and rigorously includes the effect of the local field. By including the local field, we have demonstrated that double resonance can be performed with alternating fields which are comparable in magnitude with the local field and that the technique works equally well when the abundant spin system is in the completely demagnetized state.

APPENDIX

In this appendix we will present a calculation of the cross-section time T_{IS}. Cross relaxation between spin systems has been discussed by several authors.[18] Our discussion will closely follow Schumacher's treatment as extended by Bloembergen *et al.* In fact, we will take over Schumacher's results, but neglect the spin-lattice relaxation terms which he included in his treatment.

The starting point for the development of a model is the Hamiltonian of Eq. (12),

$$\mathcal{H}'=\mathcal{H}_{ZI}+\mathcal{H}_{ZS}+\mathcal{H}_{dII}{}^0+\mathcal{H}_{dSS}{}^0+\mathcal{H}_{dIS}{}^0. \quad \text{(A1)}$$

Following Schumacher we make two assumptions:

(1) We assume the coupling between $\mathcal{H}_{ZI}$ and $\mathcal{H}_{dII}{}^0$ and between $\mathcal{H}_{ZS}$ and $\mathcal{H}_{dSS}{}^0$ is much stronger than the interactions which proceed via $\mathcal{H}_{dIS}{}^0$. Consequently the I system, described by $\mathcal{H}_I=\mathcal{H}_{ZI}+\mathcal{H}_{dII}{}^0$, can be characterized by a spin temperature θ_I, and the S system, described by $\mathcal{H}_S=\mathcal{H}_{ZS}+\mathcal{H}_{dSS}{}^0$, can be characterized by a spin temperature θ_S. (It is undoubtedly incorrect that $\mathcal{H}_{ZS}$ and $\mathcal{H}_{dSS}{}^0$ couple more strongly than $\mathcal{H}_{dIS}{}^0$, but the θ_S assumption may still hold.)

(2) We assume that the interaction between $\mathcal{H}_I$ and $\mathcal{H}_S$ due to $\mathcal{H}_{dIS}{}^0$ is a weak perturbation so that the rate of change of level populations in each system can be described by rate equations involving transition probabilities.

Letting R_{SI} and R_{IS} denote, respectively, the rate of energy flow from the S to the I system, and from the I

[18] A. Abragam and W. G. Proctor, Phys. Rev. **109**, 1441 (1958); R. T. Schumacher, *ibid.* **112**, 837 (1958); N. Bloembergen, S. Shapiro, P. S. Pershan, and J. O. Artman, *ibid.* **114**, 445 (1959); P. S. Pershan, *ibid.* **117**, 109 (1960); B. N. Provotorov, Zh. Eksperim. i Teor. Fiz. **42**, 882 (1962) [translation: Soviet Phys.—JETP **15**, 611 (1962)].

to the S system, we can write down rate equations for the cross-relaxation process in terms of the inverse spin temperatures,

$$\frac{d}{dt}\left[\frac{1}{\theta_I}\right]=-R_{IS}\left[\frac{1}{\theta_I}-\frac{1}{\theta_S}\right],$$
$$\frac{d}{dt}\left[\frac{1}{\theta_S}\right]=-R_{SI}\left[\frac{1}{\theta_S}-\frac{1}{\theta_I}\right]. \quad \text{(A2)}$$

These coupled rate equations define the R's, and are a special case of Schumacher's results. Using assumptions (1) and (2) above, Eqs. (A2) can be rigorously derived. The derivation will not be given here since it is discussed in detail by Schumacher who shows that R_{SI} and R_{IS} are given by

$$R_{SI}=\frac{\sum_{nr,ms} W_{nr,ms}(E_r-E_s)^2}{2\ \mathrm{Tr}[\mathcal{H}_S^2]\eta_I}, \quad \text{(A3)}$$

$$R_{IS}=\frac{\sum_{nr,ms} W_{ms,nr}(E_n-E_m)^2}{2\ \mathrm{Tr}[\mathcal{H}_I^2]\eta_S}, \quad \text{(A4)}$$

where $W_{ms,nr}$ is the probability per unit time for a transition between states $|m\rangle$ and $|n\rangle$ of the I system and states $|s\rangle$ and $|r\rangle$ of the S system, E_n, E_m, E_r, and E_s are, respectively, the energies of the states $|n\rangle$, $|m\rangle$, $|r\rangle$, and $|s\rangle$, $(\mathcal{H}_I|m\rangle=E_m|m\rangle)$, and η_I and η_S are, respectively, the total number of spin states of the I- and S-spin systems. Using the principles of detailed balancing and energy conservation, we find

$$\frac{R_{SI}}{R_{IS}}=\frac{\mathrm{Tr}[\mathcal{H}_I^2]\eta_S}{\mathrm{Tr}[\mathcal{H}_S^2]\eta_I}. \quad \text{(A5)}$$

In terms of the above model, equilibrium is described by $\theta_I=\theta_S$. Thus we can combine Eqs. (A2) to obtain a single equation involving the difference in the inverse spin temperatures,

$$\frac{d}{dt}\left[\frac{1}{\theta_I}-\frac{1}{\theta_S}\right]=-[R_{SI}+R_{IS}]\left[\frac{1}{\theta_I}-\frac{1}{\theta_S}\right]. \quad \text{(A6)}$$

A solution to this equation will be an exponential function with a time constant given by

$$1/T_{IS}=R_{SI}+R_{IS}. \quad \text{(A7)}$$

Using Curie's Law we then find that after a single mixing pulse, during which $(H_1)_S$ is turned on for a time t_{on}, the magnetization M of the I spins is given by

$$M=[M_i-M_f]e^{-t_{\mathrm{on}}/T_{IS}}+M_f, \quad \text{(A8)}$$

where M_i is the initial magnetization and M_f is the I magnetization at equilibrium. Equation (A8) can be combined with the results of Sec. II of the text to give the magnetization of the I spins after N mixing pulses for $\epsilon\ll 1$ as

$$M/M_i=\exp\{-N\epsilon[1-e^{-t_{\mathrm{on}}/T_{IS}}]\}, \quad \text{(A9)}$$

where

$$\frac{1}{T_{IS}}=\left[1+\frac{\mathrm{Tr}[\mathcal{H}_S^2]\eta_I}{\mathrm{Tr}[\mathcal{H}_I^2]\eta_S}\right]\frac{\sum_{nrms} W_{nr,ms}(E_r-E_s)^2}{2\ \mathrm{Tr}[\mathcal{H}_S^2]\eta_I}. \quad \text{(A10)}$$

The transition probability per unit time $W_{nr,ms}$ will be calculated using first order, time-dependent perturbation theory. In performing this calculation we assume that the I-spin "absorption line" has a Gaussian shape and the S-spin line shape is a delta function.

To calculate $W_{nr,ms}$ for the case where $(H_1)_I>H_L$ we start with the Hamiltonian

$$\mathcal{H}=\mathcal{H}_I+\mathcal{H}_S+\mathcal{H}_{dIS}^0, \quad \text{(A11)}$$

where

$$\mathcal{H}_I=-\gamma_I(H_1)_I\sum_p I_{xp}+\tfrac{1}{2}\sum_{pq} A_{pq}[3I_{zp}I_{zq}-\mathbf{I}_p\cdot\mathbf{I}_q], \quad \text{(A12)}$$

$$\mathcal{H}_S=-\gamma_S\hbar(H_1)_S\sum_j S_{xj}, \quad \text{(A13)}$$

$$\mathcal{H}_{dIS}^0=\sum_{jk} B_{jk}I_{zj}S_{zk}, \quad \text{(A14)}$$

$$A_{pq}=\tfrac{1}{2}\gamma_I^2\hbar^2\left[\frac{1-3\cos^2\theta_{pq}}{r_{pq}^3}\right], \quad \text{(A15)}$$

$$B_{jk}=\gamma_I\gamma_S\hbar^2\left[\frac{1-3\cos^2\theta_{jk}}{r_{jk}^3}\right]. \quad \text{(A16)}$$

Note that the term $\mathcal{H}_{dSS}^0$ has been dropped in Eq. (A13) since we assume the S-spin line shape to be a delta function. From first order, time-dependent perturbation theory we have

$$W_{nr,ms}=\frac{2\pi}{\hbar}|\langle n,r|\mathcal{H}_{dIS}^0|m,s\rangle|^2\times\delta(E_n+E_r-E_m-E_s). \quad \text{(A17)}$$

The quantity to be calculated is $\sum_{nrms} W_{nr,ms}(E_r-E_s)^2$. Expanding the matrix element in Eq. (A17) we find

$$\sum_{nrms} W_{nr,ms}(E_r-E_s)^2=\frac{2\pi}{\hbar}\gamma_S^2\hbar^2(H_1)_S^2\sum_{\substack{jj'kk'\\ nrms}} B_{jk}B_{j'k'}\times\langle n|I_{zk}|m\rangle\langle m|I_{zk'}|n\rangle\langle r|S_{yj}|s\rangle\langle s|S_{yj'}|r\rangle\times\delta(E_n-E_m+E_r-E_s). \quad \text{(A18)}$$

We now define a function $g_{jj'}(\omega)$ by the equation

$$g_{jj'}(\omega)=\sum_{nmkk'}\langle n|I_{zk}|m\rangle\langle mI_{zk'}|n\rangle\times B_{jk}B_{j'k'}\delta(E_n-E_m-\hbar\omega), \quad \text{(A19)}$$

where we shall soon set $|\hbar\omega|=|E_r-E_s|=|\gamma_S(H_1)_S|$.

Were the A_{pq}'s zero, the only nonvanishing matrix elements of I_{zk} would join states $\hbar\Omega_I=\gamma\hbar(H_1)_I$ apart in energy. For nonzero A_{pq} we assume, therefore,

$$g_{jj'}(\omega)=C_{jj'}[e^{-(\omega-\Omega_I)^2/\omega_1^2}+e^{-(\omega+\Omega_I)^2/\omega_1^2}], \quad \text{(A20)}$$

where $C_{jj'}$ reflects the strength of the line and ω_1 its width. This is a useful assumption since $C_{jj'}$ and ω_1^2 can be calculated exactly by the method of moments.

To evaluate $C_{jj'}$, Eqs. (A19) and (A20) are integrated over ω and equated. This gives

$$C_{jj'}=\frac{1}{2}\frac{1}{\pi^{1/2}\omega_1\hbar}\frac{I(I+1)}{3}(2I+1)^{N_I}\sum_k B_{jk}B_{j'k} \quad \text{(A21)}$$

To evaluate ω_1^2 we do a second moment calculation, i.e., using Eqs. (A19) and (A20) we evaluate the integral

$$\int_{-\infty}^{\infty}\omega^2 g_{jj'}(\omega)d\omega=\langle\omega^2\rangle\int_{-\infty}^{\infty}g_{jj'}(\omega)d\omega$$

and equate the two results.

Although $\mathcal{H}_{dII}^0$ commutes with the Zeeman Hamiltonian in the laboratory frame, it does not commute with the Zeeman Hamiltonian in the rotating frame. In carrying out the second moment calculation involving Eq. (A20) it is important to use only the secular part of the truncated dipolar interaction $\mathcal{H}_{dII}^0$. The reason for keeping only the secular part of the truncated dipolar interaction in the second moment calculation is the same as in a moment calculation in the laboratory frame.[14] The nonsecular terms correspond to weak absorption peaks at frequencies $\pm\Omega_I$ from the central absorption peak. If these satellite lines are included in a determination of the moments they give a contribution of the same magnitude as the contribution from the central peak although they have only minor influence on the cross-relaxation. Therefore, only the secular part of $\mathcal{H}_{dII}^0$ will be retained. In the present case we want only that part of $\mathcal{H}_{dII}^0$ which commutes with $\sum_p I_{xp}$. Denoting this by $\mathcal{H}_{dII}^{00}$ we find

$$\mathcal{H}_{dII}^{00}=-\tfrac{1}{4}\sum_{pq}A_{pq}[3I_{xp}I_{xq}-\mathbf{I}_p\cdot\mathbf{I}_q]. \quad \text{(A22)}$$

The integral using Eq. (A20) gives

$$\int_{-\infty}^{\infty}g_{jj'}(\omega)\omega^2 d\omega=\left[\Omega_I^2+\frac{\omega_1^2}{2}\right]\int_{-\infty}^{\infty}g_{jj'}(\omega)d\omega. \quad \text{(A23)}$$

Evaluating the same quantity using Eq. (A19) gives

$$\int_{-\infty}^{\infty}\omega^2 g_{jj'}(\omega)d\omega=\frac{1}{\hbar^3}\sum_{kk'}B_{jk}B_{j'k'}\times\mathrm{Tr}[[\mathcal{H}_I^0,I_{zk}][\mathcal{H}_I^0,I_{zk'}]],$$

where $\mathcal{H}_I^0=\mathcal{H}_{ZI}+\mathcal{H}_{dII}^{00}$. Evaluation of the trace is straightforward and gives

$$\int_{-\infty}^{\infty}g_{jj'}(\omega)[\omega^2-\Omega_I^2]d\omega=\frac{1}{\hbar^2}\frac{1}{4}\left[\frac{I(I+1)}{3}\right]^2(2I+1)^{N_I}\times\sum_{kp}5B_{jk}B_{j'k}A_{kp}^2 \quad \text{(A24)}$$

Equating Eqs. (A23) and (A24) we obtain

$$\omega_1^2=\tfrac{5}{6}I(I+1)\sum_p\left[\frac{A_{kp}}{\hbar}\right]^2, \quad \text{(A25)}$$

where the summation goes over the I spins. From the definition of A_{pq} we have

$$\sum_p\left[\frac{A_{kp}}{\hbar}\right]^2=\tfrac{1}{4}\gamma_I^4\hbar^2\frac{N_I}{N_T}\Phi,$$

where

$$\Phi=\sum_{\text{all }p}\frac{[1-3\cos^2\theta_{pk}]^2}{r_{pk}^6}$$

and N_T is the total number of spins per unit volume. Since the expression for the contribution of like spins to the second moment is[14]

$$\langle\Delta^2\omega\rangle_{II}=\tfrac{3}{4}\gamma_I^4\hbar^2 I(I+1)\frac{N_I}{N_T}\Phi,$$

we obtain

$$\omega_1^2=(5/18)\langle\Delta^2\omega\rangle_{II}. \quad \text{(A26)}$$

Thus we obtain

$$\sum_{nrms}W_{nr,ms}(E_r-E_s)^2=\frac{2\pi}{\hbar}\gamma_S^2\hbar^2(H_1)_S^2\sum_{jj'rs}C_{jj'}[e^{-(\omega-\Omega_I)^2/\omega_{12}}+e^{-(\omega+\Omega_I)^2/\omega_{12}}]\times\langle r|S_{vj}|s\rangle\langle s|S_{vj}|r\rangle.$$

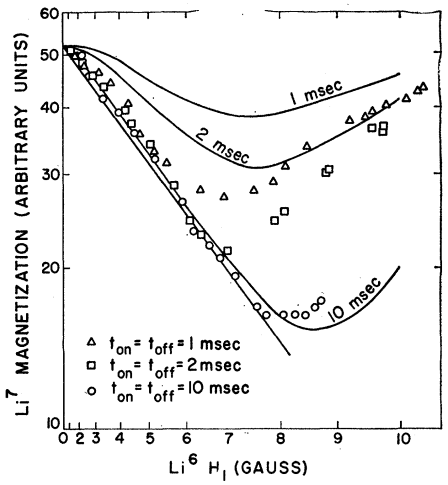

FIG. 9. $\ln M_7$ versus $(H_1)_6^2$ at 1.5°K. The solid curves are calculated using Eqs. (A9) and (A29). The solid straight line and data points are the same as in Fig. 4.

Now $\langle r|S_{yj}|s\rangle$ joins states differing in energy by $\hbar\gamma_S(H_1)_S=\hbar\Omega_S$. Thus one or the other of the exponentials is picked out which gives

$$\sum_{nrms} W_{nr,ms}(E_r-E_s)^2 = \frac{2\pi}{\hbar}\gamma_S^2\hbar^2(H_1)_S^2 e^{-(\Omega_S-\Omega_I)^2/\omega_{12}} \times\sum_{jj'}\mathrm{Tr}[C_{jj'}S_{yj}S_{yj'}]. \quad \text{(A27)}$$

Working out the trace and substituting into Eq. (A3) we find

$$R_{SI}=-\frac{4}{3}\frac{\gamma_S^2}{\gamma_I^2}\left[\frac{\pi\langle\Delta^2\omega\rangle_{II}}{10}\right]^{1/2} e^{-(\Omega_S-\Omega_I)^2/\omega_{12}}, \quad \text{(A28)}$$

where

$$\omega_1^2=(5/18)\langle\Delta^2\omega\rangle_{II},$$
$$\Omega_S=\gamma_S(H_1)_S,$$
$$\Omega_I=\gamma_I(H_1)_I.$$

Using the relationship in Eq. (A5) we obtain for the cross-relaxation time

$$\frac{1}{T_{IS}}=\left[1+\frac{N_S S(S+1)\gamma_S^2(H_1)_S^2}{N_I I(I+1)\gamma_I^2[(H_1)_I^2+\frac{1}{3}\langle\Delta^2H\rangle_{II}]}\right] \times\frac{4}{3}\frac{\gamma_S^2}{\gamma_I^2}\left[\frac{\pi\langle\Delta^2\omega\rangle_{II}}{10}\right]^{1/2} e^{-(\Omega_S-\Omega_I)^2/\omega_{12}}. \quad \text{(A29)}$$

The calculation of the cross-relaxation time in the completely demagnetized state is essentially the same as that outlined above. The major change with

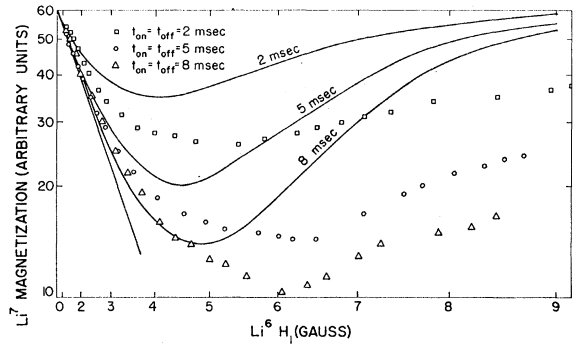

FIG. 10. $\ln M_7$ versus $(H_1)_6^2$ at 1.5°K in the completely demagnetized state. The solid curves are calculated using Eqs. (A9) and (A29). The solid straight line and data points are the same as in Fig. 7.

$(H_1)_I\ll H_L$ is that the Hamiltonian for the I-spin system is given by the dipolar term only. Thus

$$\mathcal{H}_I=\tfrac{1}{2}\sum_{pq}A_{pq}[3I_{zp}I_{zq}-\mathbf{I}_p\cdot\mathbf{I}_q]. \quad \text{(A30)}$$

Note that $\mathcal{H}_S$ and $\mathcal{H}_{dIS}^0$ are unchanged and are still given by Eqs. (A13) and (A14). Since the I-system Hamiltonian is given by the dipolar Hamiltonian, the I-spin "absorption line" is now assumed to be a single Gaussian function centered at the origin. The calculation of the second moment of this line will involve the full dipolar Hamiltonian of Eq. (A30). The calculation proceeds in the same manner as outlined above. The result for the case where $(H_1)_I\ll H_L$ is found to be

$$\frac{1}{T_{IS}}=\left[1+\frac{N_S\gamma_S^2S(S+1)(H_1)_S^2}{N_I\gamma_I^2I(I+1)\frac{1}{3}\langle\Delta^2H\rangle_{II}}\right] \times\frac{2}{3}\frac{S^2}{I^2}[\langle\Delta^2\omega\rangle_{II}]^{1/2}e^{-\Omega_S^2/\omega_{12}}, \quad \text{(A31)}$$

where now $\omega_1^2=(4/9)\langle\Delta^2\omega\rangle_{II}$.

It is important to note that Eqs. (A30) and (A31) are calculated assuming that the frequencies of the H_1's are constant and equal to the resonant frequencies of the I and S spins, and the ratio $(H_1)_S:(H_1)_I$ is varied. A calculation of the mixing time for fixed magnitudes of the H_1 fields and variation of the frequency of $(H_1)_S$ has been carried out by Hartmann and Hahn.[8] These authors perform the calculation using an expansion of the density matrix but make essentially the same assumptions (spin temperature and Gaussian line shape) which we have used in setting up our model. Equations (A30) and (A31) can be combined with Eq. (A9) and compared with the experimental data of Figs. 4 and 7. The results are shown in Figs. 9 and 10. In both cases we see that the experimental mixing takes place faster than the mixing calculated on the basis of our simple model.

In particular, some preliminary results on the measurement of the cross-relaxation time indicate that more than one relaxation rate is involved in the mixing whereas the simple model we have used to calculate the cross-relaxation assumes a single relaxation rate between the two spin systems. Thus, although the calculated curves do tend to reflect the general form of the experimental results, it is not surprising that the agreement between theory and experiment is only qualitative.